

Modeling Platinum Group Metal Complexes in Aqueous Solution

Achim Lienke,[†] Günter Klatt, David J. Robinson, Klaus R. Koch,[‡] and Kevin J. Naidoo*

Department of Chemistry, University of Cape Town, Rondebosch 7701, South Africa

Received May 31, 2000

We construct force fields suited for the study of three platinum group metals (PGM) as chloranions in aqueous solution from quantum chemical computations and report experimental data. Density functional theory (DFT) using the local density approximation (LDA), as well as extended basis sets that incorporate relativistic corrections for the transition metal atoms, has been used to obtain equilibrium geometries, harmonic vibrational frequencies, and atomic charges for the complexes. We found that DFT calculations of $[\text{PtCl}_6]^{2-} \cdot 3\text{H}_2\text{O}$, $[\text{PdCl}_4]^{2-} \cdot 2\text{H}_2\text{O}$, and $[\text{RhCl}_6]^{3-} \cdot 3\text{H}_2\text{O}$ water clusters compared well with molecular mechanics (MM) calculations using the specific force field developed here. The force field performed equally well in condensed phase simulations. A 500 ps molecular dynamics (MD) simulation of $[\text{PtCl}_6]^{2-}$ in water was used to study the structure of the solvation shell around the anion. The resulting data were compared to an experimental radial distribution function derived from X-ray diffraction experiments. We found the calculated pair correlation functions (PCF) for hexachloroplatinate to be in good agreement with experiment and were able to use the simulation results to identify and resolve two water–anion peaks in the experimental spectrum.

1. Introduction

The dynamics of transition metal complexes in solution can be investigated using computer modeling, if the electronic structures of both complex and solvent can be accurately represented and the simulation covers a sufficiently long time span. With the ongoing increase in computing power and the advent of fully ab initio molecular dynamics (MD) computer simulations, computing the metal complex–solvent interaction to a high degree of accuracy is already feasible.¹ However, the length of these ab initio simulations is restricted to a few picoseconds, which prohibits sufficient sampling of phase space necessary for the calculation of solution properties such as diffusion constants. A classical force field approach, derived from both experimental measurements and quantum chemical calculations, may be used to increase the simulation time.² We used the latter procedure to study solvent structuring around several platinum group metal (PGM) complexes.

One of the defining features of PGM chemistry in aqueous solution containing chloride anions is the tendency of the metal cations to form stable and kinetically inert octahedral $[\text{MCl}_6]^{n-}$ or square-planar $[\text{MCl}_4]^{2-}$ complexes. Thus Pt(IV) and Rh(III) exist mainly as $[\text{PtCl}_6]^{2-}$ and $[\text{RhCl}_6]^{3-}$ in hydrochloric acid solution, while Pt(II) and Pd(II) form $[\text{PtCl}_4]^{2-}$ and $[\text{PdCl}_4]^{2-}$ species.³ A model of these metal complexes in solution cannot be complete without a physically acceptable description of the bond stretching motion. The halogen–PGM complexes are relatively rigid molecules; consequently, these complexes can

be reasonably described by a multidimensional harmonic oscillator potential function. The parameters contained in the potential function can be fitted to reproduce experimental observables of a library of molecules. In this respect a complete vibrational analysis for K_2PtCl_6 has been reported, which includes the silent modes.⁴ Furthermore, incomplete sets of vibrational frequencies for $[\text{PdCl}_4]^{2-}$ and $[\text{RhCl}_6]^{3-}$ have been determined.³

Theoretical electronic structure calculations have been performed on several PGM chloranions.^{5,6} These authors used density functional theory (DFT) methods in order to examine the transition state of ligand substitution in square planar PGM complexes.

We are concerned with the development of models that will accurately reproduce the structure and behavior of PGM chloranions in solution. For this purpose X-ray diffraction, along with neutron diffraction experiments, provides the most information on metal complexes in a solvent environment, against which the performance of our models can be compared. However, a survey of the literature revealed only very few such studies. X-ray scattering measurements of $[\text{PtCl}_6]^{2-}$ solutions have been conducted to investigate the geometry of hexachloroplatinate(IV) in an aqueous environment.⁷ In addition to the geometry, the authors obtained data which they concluded to be evidence of local water structuring around the metal complex, although they did not elaborate on the data, since their experiments were not designed to probe this aspect of the solution structure. More recently, X-ray diffraction experiments have been used to examine $[\text{PdCl}_4]^{2-}$ and $[\text{PtCl}_4]^{2-}$ aqueous solutions.⁸ In this paper, we shall concentrate on demonstrating

* To whom correspondence should be addressed. E-mail: knaidoo@psipsy.uct.ac.za.

[†] Current address: Unilever Research Vlaardingen, Oliver van Noortlaan 120, 3133 AT Vlaardingen, The Netherlands.

[‡] Current address: Department of Chemistry, University of Stellenbosch, 7602 Stellenbosch, South Africa.

(1) Carloni, C.; Sprik, M.; Andreoni, W. *J. Phys. Chem.* **2000**, *104*, 823–835.

(2) Villa, A.; Cosentino, U.; Pitea, D.; Moro, G.; Maiocchi, A. *J. Phys. Chem. A* **2000**, *104*, 3421–3429.

(3) Cotton, S. A. *Chemistry of Precious Metals*; Chapman & Hall: London, 1997.

(4) Parker, S. F.; Forsyth, J. B. *J. Chem. Soc., Faraday Trans.* **1998**, *94*, 1111–1114.

(5) Deeth, R. J. *Chem. Phys. Lett.* **1996**, *261*, 45–50.

(6) Deeth, R. J.; Elding, L. I. *Inorg. Chem.* **1996**, *35*, 5019–5026.

(7) Maeda, M.; Aksishi, T.; Ohtaki, H. *Bull. Chem. Soc. Jpn.* **1975**, *48*, 3193–3196.

(8) Camintiti, R.; Carbone, M.; Sadun, C. *J. Mol. Liq.* **1998**, *75*, 149–158.

the accuracy of our model for $[\text{PtCl}_6]^{2-}$ solutions, because the published experimental data on this species are the most complete of all of the PGM chlorocomplexes studied by us.

The CHARMM program has been primarily designed for simulating biopolymers.⁹ It has an extensive parameter set for the treatment of organic monomers but does not contain any parameters for transition metal complexes. We have recently added a chromium organometallic force field¹⁰ and are currently extending this force field to include numerous transition metal complexes and organometallic systems. There are existing molecular mechanics (MM) force fields that have been developed for the design of platinum compounds with anticancer activity¹¹ and organometallic complexes.¹² These force fields are mostly used for calculations in vacuo and sometimes in the solid state. However, to our knowledge there is no force field for PGM chloranions that can be applied to model solution environments, in particular water.

In section 2 we present the details of the quantum mechanical and MD calculations. The force field is presented and discussed in section 3. The resultant MM models were tested against (a) DFT metal complex–water interaction calculations and (b) experimental PGM chloroanion hydration shell X-ray diffraction data (sections 4 and 5).

2. Computational Details

2.1 DFT Calculations. Geometry, harmonic potential, and electron densities of the PGM complexes were obtained using density functional theory as implemented in the GAUSSIAN94 program.¹³ Octahedral symmetry (point group O_h) was found for $[\text{PtCl}_6]^{2-}$ and $[\text{RhCl}_6]^{3-}$, and a square planar geometry (point group D_{4h}) for $[\text{PdCl}_4]^{2-}$. We found that the gradient-corrected DFT functionals severely overestimated the M–Cl bond lengths, while the LDA method, using the correlation functional by Vosko, Wilk, and Nusair (VWN)¹⁴ and Slater's exchange functional,¹⁵ produced bond lengths that are in good agreement with experiment. Hay–Wadt LanL2DZ basis sets¹⁶ were used for the metal centers, which include relativistic corrections via effective core potentials, and a 6-31+G(2d) basis set on the chloride ligands, giving a total of 184 basis functions. These observations are in agreement with the findings of Deeth et al. for PGM chloranions.^{5,6}

In general, the parameters regulating bond strengths in molecular harmonic force fields are best derived from experimental data, which may be based on infrared and Raman spectroscopy. However, only a subset of the vibrational frequencies is currently available for most of the PGM chloranions. Consequently we resorted to calculating the harmonic frequencies using DFT methods. The above-mentioned approach was used to produce a full set of vibrational frequencies for $[\text{PtCl}_6]^{2-}$ and $[\text{RhCl}_6]^{3-}$. Since the calculated frequencies differ from

experiment by a constant of 27 cm^{-1} , we added this value to our computed frequencies instead of the upward scaling procedure commonly used for quantum mechanically derived values. The resulting frequencies are mostly within 10 cm^{-1} of the experimental values and therefore in good agreement. This is further evidence that the LDA approximation gives a realistic description of the electron densities of the complexes studied.

In this study we derive point charges fitted to the quantum mechanically produced electrostatic potential (ESP) at points selected according to the Merz–Kollman–Singh scheme.¹⁷ This approach to calculating atomic charges has been shown to give reliable results for electrostatic interaction due to large effective van der Waals exclusion radii.¹⁸ In the Merz–Kollman–Singh scheme the quantum mechanically produced ESP is calculated at a number of Connolly molecular surfaces.¹⁹ These surfaces are generated as a function of multiples (1.4–2.0) of the van der Waals radii of the component atoms. The classical ESP surfaces are calculated from the point charge model as constructed by assigning partial charges to the atoms. These are then least-squares fitted to the quantum surfaces, generated from the electronic wave function, with the constraint that the net charge on the molecule is reproduced. Recently, Hambley proposed van der Waals values for the Pt(II) and Pd(II) cations²⁰ which agree well with those published by Bondi.²¹ We similarly used van der Waals radii of 1.70 \AA for all the PGM cations. We have been unable to find any values for Rh(III) and Pt(IV) in the literature. Consequently we calculated a number of Merz–Kollman–Singh charges for $[\text{PtCl}_6]^{2-}$ and $[\text{RhCl}_6]^{3-}$ using van der Waals radii ranging from 1.5 to 2.6 \AA for the metal ions and found that the charges assigned to the PGMs remained constant for radii below 2.0 \AA . The reason for this is that the metal ions are buried inside the octahedral complexes and have no effect on the shape of the Connolly surface when they are smaller than 2.0 \AA ; as a result, the partial charge assignments remain unchanged. Since it is unlikely that the van der Waals radii of Rh(III) and Pt(IV) would be larger than the 1.70 \AA found for the Pt(II) and Pd(II) cations, we believe that our choice of van der Waals radii for the PGMs is reasonable.

A different DFT functional was used for the PGM complexes and water when calculating complex–solvent interaction. Recently a study of water–anion interactions has established B3LYP as the best functional for such calculations.²² This functional consists of the correlation energy functional of Lee, Young, and Parr²³ and Becke's three parameter hybrid correction.²⁴ The LanL2DZ basis was again used for the metal centers, and a 6-311++G(2d,2p) basis set for all other atoms. The basis set superposition error (BSSE) was estimated by the counterpoise correction. For the PGMs this involves delocalization of charge and, therefore, is quite considerable. We estimated the amount of binding that was due to the BSSE by placing ghost orbitals on the chlorine atoms only. Since a high-level basis set was used, the total electronic wave function for the waters was well described with our basis, and the BSSE turned out to be comparatively small, consisting of merely 0.5% of the total binding energy.

2.2 MM/MD Computational Details. A peculiarity of coordination compounds is the extreme flexibility of valence angles involving the metal centers, resulting in comparatively small force constants for the description of angular distortion between metal center and coordinated ligands. To account for electronically related deviations from tetrahedral and octahedral geometries, a number of distortion potentials have been developed and successfully applied.^{25–29} As a basis for our own

- (9) Brooks, B. R.; Bruccoleri, R. E.; Olafson, B. D.; States, D. J.; Swaminathan, S.; Karplus, M. *J. Comput. Chem.* **1983**, *4*(2), 187–217.
- (10) Hughes, S. J.; Moss, J. R.; Naidoo, K. J.; Kelley, J. F.; Batsanov, A. S. *J. Organomet. Chem.* **1999**, *588*, 176–185.
- (11) Yao, S.; Plastaras, J. P.; Marzilli, L. G. *Inorg. Chem.* **1994**, *33*, 6061–6077.
- (12) Rappe, A. K.; Colwell, K. S.; Casewit, C. J. *Inorg. Chem.* **1993**, *32*, 3438–3450.
- (13) Frisch, M. J.; Trucks, G. W.; Schlegel, H. B.; Gill, P. M. W.; Johnson, B. G.; Robb, M. A.; Cheeseman, J. R.; Keith, T. A.; Petersson, G. A.; Montgomery, J. A.; Raghavachari, K.; Al-Laham, M. A.; Zakrzewski, V. G.; Ortiz, J. V.; Foresman, J. B.; Cioslowski, J.; Stefanov, B. B.; Nanayakkara, A.; Challacombe, M.; Peng, C. Y.; Ayala, P. Y.; Chen, W.; Wong, M. W.; Andres, J. L.; Replogle, E. S.; Gomperts, R.; Martin, R. L.; Fox, D. J.; Binkley, J. S.; Defrees, D. J.; Baker, J.; Stewart, J. P.; Head-Gordon, M.; Gonzalez, C.; Pople, J. A. *Gaussian 94*, revision D.3; Gaussian Inc.: Pittsburgh, PA, 1995.
- (14) Vosko, S. H.; Wilk, L.; Nusair, M. *Can. J. Phys.* **1980**, *58*, 1200–1211.
- (15) Slater, J. C. *Quantum Theory of Molecules and Solids*; McGraw-Hill: New York, 1974; Vol. 4.
- (16) Wadt, W. R.; Hay, P. J. *J. Chem. Phys.* **1985**, *82*, 284–298.

- (17) Bessler, B. H.; Merz, K. M.; Kollman, P. A. *J. Comput. Chem.* **1990**, *11*, 431–439.
- (18) Sigfridsson, E.; Ryde, U. *J. Comput. Chem.* **1998**, *19*, 377–395.
- (19) Connolly, M. *Connolly Surfaces for Molecules*; Connolly, M., Ed.; Quantum Chemistry Program Exchange: Bloomington, IN, 1982.
- (20) Hambley, T. W. *Inorg. Chem.* **1998**, *37*, 3767–3774.
- (21) Bondi, A. *J. Phys. Chem.* **1964**, *68*, 441–451.
- (22) Pudzianowski, A. T. *J. Phys. Chem.* **1996**, *100*, 4781–4789.
- (23) Lee, C.; Yang, W.; Parr, R. G. *Phys. Rev. B* **1988**, *37*, 785–789.
- (24) Becke, A. D. *J. Chem. Phys.* **1993**, *98*, 5648–5652.
- (25) Burton, V. J.; Deeth, R. J. *J. Chem. Soc., Chem. Commun.* **1995**, 573–574.
- (26) Sabolovic, J.; Raos, N. *Polyhedron* **1990**, *9*, 1277–1286.
- (27) Sabolovic, J.; Raos, N. *Polyhedron* **1990**, *9*, 2419–2427.
- (28) Comba, P. *Inorg. Chem.* **1985**, *24*, 2325–2327.

modeling effort, we chose a force field based on a modified Urey–Bradley approach.³⁰

In this model, the coordination geometry is a consequence of ligand–ligand nonbonded interactions. Consequently, our MM model excludes the valence angle bending terms from the potential energy expression. Instead, we use 1,3 nonbonded interaction terms for the forces acting between ligand atoms, involving both van der Waals and electrostatic interactions. A similar approach, in which only the van der Waals terms were included, has previously been shown to yield more reliable results compared to an energy expression containing only a single bending term (i.e. without cross terms).³¹

A possible reason for this lies in our observation that those vibrational frequencies resulting from this simple harmonic expression do not have the correct degeneracy. The nonbonded interactions (both van der Waals and electrostatic terms) between the chloride ligands were modeled using the standard expression given in Eq 1.

The parameters ϵ , σ , and R_{ij} are the van der Waals well depth, van der Waals collision diameter, and the equilibrium atomic distance between atoms i and j , while q_i and q_j are the atomic charges for atoms i and j , respectively.

$$E_{\text{nb}} = \sum_{ij} 4\epsilon \left[\left(\frac{\sigma}{R_{ij}} \right)^{12} - \left(\frac{\sigma}{R_{ij}} \right)^6 \right] + \sum_{ij} \left(\frac{q_i q_j}{4\pi\epsilon_0 R_{ij}} \right) \quad (1)$$

For electronic reasons, low-spin d^6 metals, such as Pt(IV) and Rh(III), display a preference to adopt an octahedral coordination and d^8 systems, such as Pd(II), favor a square planar coordination. In the case of simple ligands, such as the chloride anion, the nonbonded 1,3 interactions among the ligands are sufficient to model the octahedral geometry of d^6 metals. However, if only the 1,3 nonbonded terms are used for a d^8 metal, a tetrahedral geometry will result. A VSEPR model that disregards the presence of free electron pairs cannot possibly work for such tetracoordinate complexes. Adding only cis (90°) angle terms in order to correct for this shortcoming can lead to highly unusual geometries. Consequently, we used an established method, whereby an improper torsion term is introduced to maintain the planarity ($\omega_0 = 0^\circ$) of the $[\text{PdCl}_4]^{2-}$ complex with a quadratic distortion constant k_ω as described in Eq 2.³²

$$E_\omega = k_\omega (\omega - \omega_0)^2 \quad (2)$$

In addition, we derived parameters describing the bond stretching motion to correlate best with scaled DFT frequencies. In most MM models, the bond stretching motions are described by a harmonic potential function, wherein r_0 is the reference bond length and k_i is the bond specific force constant observed experimentally (Eq 3).

To maintain metal–ligand bond lengths and vibrational frequencies that are consistent with experimental (or ab initio) values, the position of the reference r_0 value and force constant k_i will vary on the basis of the strength of the repulsive force of the interacting ligands. This is because the 1,3 nonbonded interactions were included in the present model and consequently r_0 and k_i no longer have their usual relation (viz. equilibrium bond length and bond stretching constant) to experiment. The equilibrium bond lengths computed in our systems are determined by the sum of the harmonic bond potentials and the interligand interaction potentials. The CHARMM program⁹ was used for all the MM and MD calculations presented here.

$$E_b = \sum_i k_i (r - r_0)^2 \quad (3)$$

To test the force field, we performed a simulation of $[\text{PtCl}_6]^{2-}$ in aqueous solution. The complex was placed in a cubic box with a side length of 24.5662 Å of previously equilibrated water. A total of 496

Table 1. M–Cl Bond Lengths for the PGM Chloranions in Å, Where “MM” Are MM Distances, “DFT” Are LDA Values, and “Exptl” are the Experimental (CSD) Results

	$[\text{PtCl}_6]^{2-}$	$[\text{PdCl}_4]^{2-}$	$[\text{RhCl}_6]^{3-}$
MM	2.315	2.307	2.349
DFT	2.347	2.329	2.382
Exptl	2.315 ± 0.008	2.307 ± 0.012	2.349 ± 0.007

water molecules were used to give a density of 1.051 g/mL. For the solvent, the TIP3P water model was used as implemented in CHARMM.^{33,34} Two sodium counterions were added in order to create a zero overall charge. We used the Ewald summation method to calculate electrostatic interactions while periodic boundary conditions were applied to simulate bulk solution. We truncated the nonbonded interactions smoothly from 8.0 to 12.0 Å using the force switch method.³⁵ The trajectories were integrated using a Verlet integration algorithm³⁶ with a step size of 1 fs. Chemical bond lengths involving hydrogen atoms and the geometries of the water molecules were kept rigid using the constraint algorithm SHAKE.³⁷ The atomic velocities were periodically scaled for 50 ps of equilibrium dynamics to maintain the system temperature at 300 K. The data were then collected over 500 ps of dynamics, during which time box size and particle number were kept constant. The temperature fluctuated around 300 K, and the total energy was well conserved.

3. Force Field Parametrization

Molecular mechanics force fields often assume transferability of parameters between molecules with common substructures. Because of quantum effects, such as ligand-specific trans influence, and different electrostatic conditions for each complex, we did not attempt to introduce transferable parameters for M–L bonds but instead parametrized each anion separately. Only the van der Waals parameters, taken from Allinger’s MM3 force field,^{38,39} and a recent study on square-planar PGM complexes,²⁰ were kept constant. Since our interest is focused on modeling PGM complexes in solution, we place a high priority on the accuracy of the frequency calculations and the molecular electrostatic profile of the metal complexes. Consequently, a highly specific force field with atomic charges and bond distortion parameters obtained from DFT calculations, bond lengths from crystallographic data, and van der Waals radii from an existing parameter set was constructed.

3.1. Force Constants and Reference Bond Lengths. The bond lengths obtained from density functional theory are slightly longer than those obtained experimentally (see Table 1). Calculating the intramolecular distances to an accuracy of 0.03 Å is excellent compared to the accuracy commonly achieved by DFT calculations.⁴⁰ However, such a deviation is quite significant when compared to the experimental structural differences among the PGM chloroanions. To obtain reliable bond length parameters, we therefore did not use the values computed with the LDA method but instead searched the Cambridge Structural Database (CSD)⁴¹ for all structures containing the anions $[\text{PdCl}_4]^{2-}$, $[\text{PtCl}_6]^{2-}$, and $[\text{RhCl}_6]^{3-}$. Since

(29) Allured, V. S.; Kelly, C. M.; Landis, C. R. *J. Am. Chem. Soc.* **1991**, *113*, 1–12.

(30) Hambley, T. W.; Hawkins, C. J.; Palmer, J. A.; Snow, M. R. *Aust. J. Chem.* **1981**, *34*, 45–56.

(31) Comba, P. *Coord. Chem. Rev.* **1993**, *123*, 1–48.

(32) Hambley, T. W. *Inorg. Chem.* **1988**, *27*, 1073–1077.

(33) Jorgensen, W. L.; Chandrasekhar, J.; Madura, J. D.; Impey, R. W.; Klein, M. L. *J. Chem. Phys.* **1983**, *79*, 926–935.

(34) Steinbach, P. J.; Brooks, B. R. *Proc. Natl. Acad. Sci. U.S.A.* **1993**, *90*, 9135–9139.

(35) Steinbach, P. J.; Brooks, B. R. *J. Comput. Chem.* **1993**, *15*, 667–683.

(36) Verlet, L. *Phys. Rev.* **1967**, *159*, 98–103.

(37) van Gunsteren, W. F.; Berendsen, H. J. C. *Mol. Phys.* **1977**, *34*, 1311–1327.

(38) Allinger, N. L. *J. Am. Chem. Soc.* **1977**, *99*, 8127–8134.

(39) Burkett, U.; Allinger, N. L. *Molecular Mechanics*; American Chemical Society: Washington, DC, 1982.

(40) Ziegler, T. *Density Functional Methods in Chemistry and Material Science*; Ziegler, T., Ed.; Wiley & Sons: New York, 1997.

(41) Allen, F. H.; Kennard, O. *Chem. Des. Autom. News* **1993**, *8*, 1, 31.

Table 2. Vibrational Frequencies for the PGM Chloranions in cm^{-1} , with “MM” as MM Wavenumbers, “DFT” as Scaled LDA Harmonic Frequencies, and “Exptl” as Experimental Measurements

	freq	MM	DFT	exptl
[PtCl ₆] ²⁻	A _{1g}	361	348	346
	T _{1u}	350	337	346
	E _g	290	326	325
	T _{1u}	176	187	183
	T _{2g}	160	161	164
	T _{2u}	114	152	147
[PdCl ₄] ²⁻	E _u	364	336	337
	A _{1g}	327	310	309
	B _{1g}	266	284	284
	E _u	159	180	
	A _{2u}	206	175	
	B _{2g}	190	173	
	B _{2u}	101	102	
[RhCl ₆] ³⁻	A _{1g}	324	297	302–308
	T _{1u}	315	306	312
	E _g	236	276	
	T _{1u}	201	183	
	T _{2g}	181	157	
	T _{2u}	113	144	

the metal–ligand bond lengths and angles are known to be sensitive to the crystal environment,⁴² these structural parameters, gained both from X-ray and neutron diffraction data, varied significantly. We selected only structures where the average M–Cl distance was within two standard deviations of the total sample average of bond lengths from all CSD PGM chloranion structures. This procedure yielded 27 structures for [PtCl₆]²⁻, 17 structures for [PdCl₄]²⁻, and 8 structures for [RhCl₆]³⁻. The experimentally derived bond lengths and standard deviations are listed in Table 1. The MM reference bond lengths (r_0) and stretching constants (k_i) were varied under the constraint that the experimentally observed bond lengths be reproduced (Table 1).

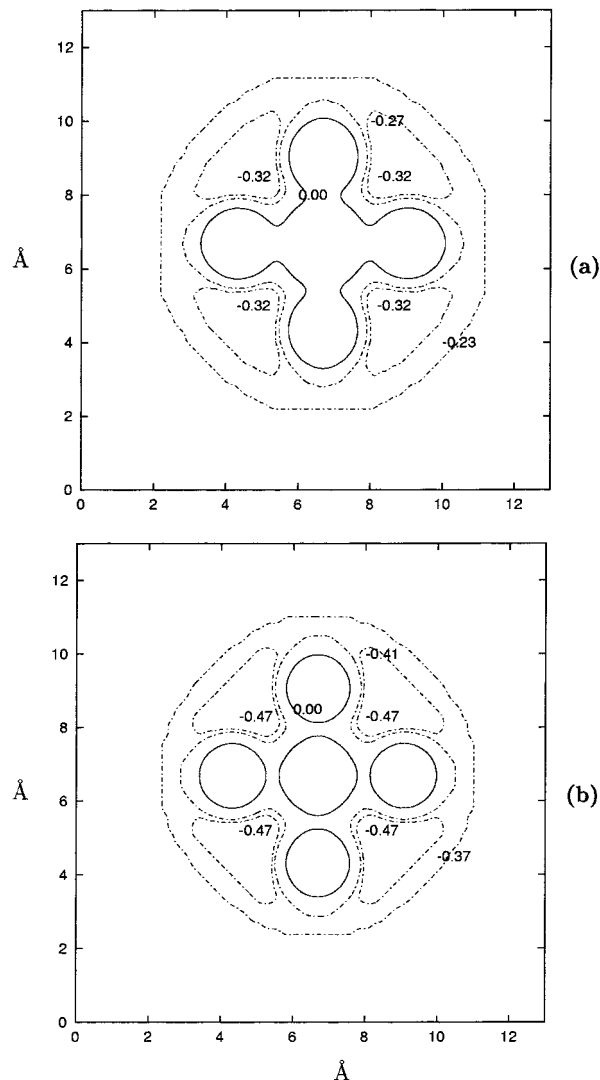
The variation of the magnitudes of the atomic charges has a strong influence on the vibrational frequencies calculated from a MM normal-mode analysis. However, manipulating the charges to achieve a better fit of the frequencies does not enhance the quality of the frequency calculation, namely the gap between the T_{1u} and E_g modes. As a result we did not vary atomic charges to improve frequency calculations. As stated above, we place prime importance on the correct reproduction of the vibrational harmonic frequencies. Therefore, our force field was chosen so that the CHARMM-produced frequencies correspond to the values from our DFT calculations. A comparison of these can be found in Table 2. The overall agreement of our MM wavenumbers with those from either experiment or DFT calculations is good. As is discussed in section 3.2 the charge on the chlorides on the rhodium complex is significantly higher than that on the platinum complex; consequently, the inter-chloride electrostatic repulsive force is much larger in the case of the former. The result is that the chlorides are pushed further out into space in the rhodium complex. Therefore, to reproduce the experimental/ab initio geometry and frequencies for the [RhCl₆]³⁻ complex, the bond parameters (r_0 and k_b) were set at considerably smaller values (Table 3) compared to those of the other two complexes.

3.2. Electrostatic Parameters. The results of our Merz–Kollman–Singh-derived charges from the quantum mechanical electrostatic potential, along with the other force field parameters, are summarized in Table 3. What is immediately striking is the difference in the charges assigned to the Pt (+0.370) and

Table 3. Force Field Parameters for the PGM Chloranions^a

param	[PtCl ₆] ²⁻	{PdCl ₄ } ²⁻	[RhCl ₆] ³⁻
R_0	2.134	2.158	1.797
k_b	110	95	70
k_w		54	
$q(\text{M})$	0.370	0.328	1.584
$q(\text{Cl})$	-0.395	-0.582	-0.764
$\epsilon(\text{Cl})$	-0.24	-0.24	-0.24
$\sigma(\text{Cl})$	2.03	2.03	2.03
$\epsilon(\text{M})$	-0.20	-0.20	-0.20
$\sigma(\text{M})$	1.70	1.70	1.70

^a Reference bond lengths R_0 and van der Waals bond lengths R_{min} in Å, bond stretching harmonic force constants k_b in $\text{kcal } \text{Å}^{-2} \text{mol}^{-1}$, charges q in units of electron charge e , and van der Waals energies ϵ_{mon} in kcal mol^{-1} .

**Figure 1.** DFT electrostatic potential in units of electron charge e for (a) [PtCl₆]²⁻ and (b) [RhCl₆]³⁻. Shown is a contoured slice corresponding to one of the σ_h planes of symmetry.

Rh (+1.584) metal ions in the [MCl₆]^{x-} octahedral complexes ($x = 2$ and 3 , respectively). However, this can be understood by investigating the quantum mechanically derived molecular ESPs for the two complexes (Figure 1). The contour lines around the chloride ligands are considerably more negative for the rhodium complex than for the platinum complex; the respective global minima being -0.45 and -0.32 e . The result is that the Merz–Kollman–Singh scheme (see section 2.1) produced partial charges that are almost two times more negative on the

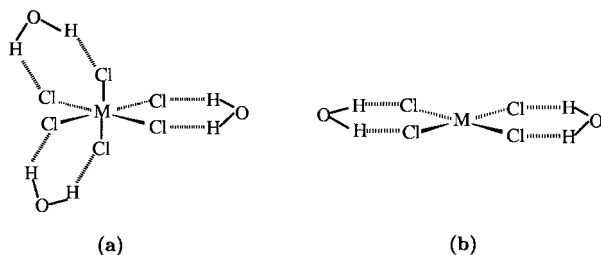


Figure 2. Illustration of the anion–water cluster structures calculated to test the force field: left, $[\text{PtCl}_6]^{2-} \cdot 3\text{H}_2\text{O}$, $[\text{RhCl}_6]^{3-} \cdot 3\text{H}_2\text{O}$; right, $[\text{PdCl}_4]^{2-} \cdot 2\text{H}_2\text{O}$.

Table 4. Comparison of DFT(B3LYP) and MM $\text{H}\cdots\text{Cl}$ Hydrogen Bond Lengths, r_{MCl} M–Cl Distances (both in Å), E_{int} Interaction Energies, BSSE, and E_{corr} Total Binding Energies (All in kcal/mol) for Three Anion–Water Clusters^a

		$\text{H}\cdots\text{Cl}$	r_{MCl}	E_{int}	BSSE	E_{corr}
$[\text{PtCl}_6]^{2-}$	DFT	2.461		42.54	2.27	40.28
	MM	2.40	2.309			53.27
		2.46	2.307			
$[\text{PdCl}_4]^{2-}$	DFT	2.377		35.54	1.40	34.15
	MM	2.300	2.301			46.30
$[\text{RhCl}_6]^{3-}$	DFT	2.344		69.49	2.75	66.74
	MM	2.276	2.339			77.40

^a The Pt cluster is found to be slightly asymmetric in the MM calculation; hence, two sets of bond lengths exist.

chlorides in the rhodium complex (-0.764 e) than the chlorides in the platinum complex (-0.395 e). Unfortunately a simple point charge model constrained by the restriction that the overall molecular charge remains constant results in the unusually large assignment of positive charge on the buried rhodium. This is to be expected since the atoms near the surface mainly determine the ESP experienced outside the molecule. This is a well-recognized weakness of a point charge model and can be addressed by adding nonnuclear centered charges at the expense of computational efficiency.^{43,44} However, since a key use of this force field is to model the behavior of these PGM complexes in solution, the Merz–Kollman–Singh charges were used so that the classical ESP closely approximated the quantum mechanically produced one (see section 2.1).

4. Comparative MM and DFT Study of Water Ion Clusters

A comparative DFT and MM study on the structures of three anion–water clusters (see Figure 2) was performed. Generally LDA is reported to overestimate interaction energies and underestimate hydrogen bond lengths.⁴⁵ We therefore decided to make use of gradient-corrected DFT, which has proven to predict structures and interaction energies of intermolecular hydrogen bonds that are in good agreement with experiment or high-level ab initio calculations.^{45–48} The MM calculations did not include a special hydrogen bond term; instead hydrogen bond behavior has been included in the nonbonded parameters of the TIP3P model.³³ The bond lengths and interaction energies obtained in this way are compared against the DFT results in Table 4. It can be seen that $\text{H}\cdots\text{Cl}$ hydrogen bond lengths produced with MM are in excellent agreement (within 0.07 Å)

with the DFT values. However, the MM interaction energies are much larger than the DFT results. The reason for this is the manner in which the water model is implemented in CHARMM³⁴ rather than our PGM chloroanion force field. The water dimer has been studied experimentally, and an interaction energy of 5.4 ± 0.7 kcal/mol is currently proposed.⁴⁹ With CHARMM-implemented TIP3P, however, an energy of 6.95 kcal/mol is obtained. Both DFT(B3LYP) and perturbation theory at the MP2 level predict an interaction energy around 4.5 kcal/mol,⁴⁸ which appears to be too low. The TIP3P and B3LYP values differ by over 55% even for a system as simple as the water dimer. The magnitude of interaction energy discrepancy between DFT and MM results is therefore not surprising.

5. Condensed Phase Aqueous Behavior of PGM Chloranions

Important benchmarks for judging the validity of any solution model are structural data derived from X-ray and neutron diffraction experiments. It is unfortunate that such studies have not been carried out for all three PGM chloranions. However, the X-ray diffraction work of Maeda et al. on the hexachloroplatinate(IV) complex⁷ provides very useful data against which to compare the quality of our model. The platinum concentration of their experimental solution was 2.8 g/L, compared to a density of 21.8 g/L of our simulated solution. Both of these correspond to rather dilute solutions, in which interactions between dissolved anions may be expected to play a negligible role. An overall radial distribution function (RDF) was determined from the scattering function. This data set was then used to solve the structure of the $[\text{PtCl}_6]^{2-}$ complex in solution. The Pt–Cl bond lengths of 2.33 Å and average cis- and trans- $\text{Cl}\cdots\text{Cl}$ distances of 3.30 and 4.66 Å, respectively, compare well with the values of 2.30 , 3.22 , and 4.58 Å from our MD simulation.

The structures of metal complexes in solution serve as a useful comparison with solid-state derived structures, in which matrix effects on the complex may be identified. However, the structuring of the water around the $[\text{PtCl}_6]^{2-}$ complex is of greater interest to us as we attempt to understand the nature of the solvation. Here the X-ray diffraction experiment is unable to describe the solvent–metal complex arrangement unambiguously because the experimental RDF includes positional correlations for a number of atom pairs, namely $\text{Pt}\cdots\text{O}$, $\text{Pt}\cdots\text{H}$, $\text{Cl}\cdots\text{O}$, and $\text{Cl}\cdots\text{H}$. Experimentally, this combination of scattering factors could only be disentangled through combined data from both X-ray and isotope labeled neutron diffraction studies. None of the additional experimental data could be found in the literature. Consequently, the two peaks around 3.2 and 4.9 Å from the experimental RDF⁷ remained unassigned.

To address the issue of assigning these peaks, separate $\text{Cl}\cdots\text{O}$, $\text{Cl}\cdots\text{H}$, $\text{Pt}\cdots\text{O}$, and $\text{Pt}\cdots\text{H}$ pair correlation functions (PCF's) were calculated from our 500 ps $[\text{PtCl}_6]^{2-}$ solution MD simulation (Figure 3). The radially averaged PCF between two atoms is defined in eq 4, where r is the interatomic distance between atoms α and β , ρ is the number density of atoms β , and $N_{\alpha\beta}(r)$ is the number of atoms β within a sphere of radius r around atom α .

The factor $(4\pi\rho r^2)^{-1}$ normalizes $g_{\alpha\beta}(r)$ to unity for large interatomic distances. The metal complex–water arrangement is best understood by studying the $g_{\text{ClO}}(r)$ functions (Figure 3 and Table 5). The $\text{Cl}\cdots\text{O}$ distribution in solution has two distinct probability peaks. The first sharp peak, centered at approxi-

(43) Aleman, C.; Orozco, M.; Luque, F. J. *Chem. Phys.* **1994**, *189*, 573.

(44) Koch, U.; Egert, E. *J. Comput. Chem.* **1995**, *16*, 937.

(45) Florian, J.; Johnson, B. G. *J. Phys. Chem.* **1995**, *99*, 5899–5908.

(46) Jeanvoine, Y.; Bohr, F.; Ruiz-Lopez, M. F. *Can. J. Chem.* **1995**, *73*, 710–715.

(47) Han, W. G.; Suhai, S. *J. Phys. Chem.* **1996**, *100*, 3942–3949.

(48) Novoa, J. J.; Sosa, C. *J. Phys. Chem.* **1995**, *99*, 15837–15845.

(49) Pine, A. S.; Howard, B. J. *J. Chem. Phys.* **1986**, *84*, 590–596.

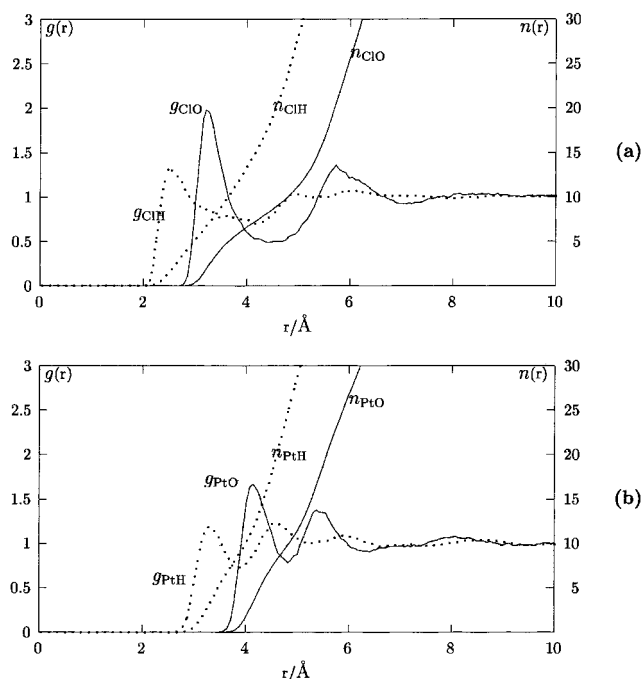


Figure 3. Pair correlation functions $g(r)$ and running integration numbers $n(r)$ for $[\text{PtCl}_6]^{2-}$ in aqueous solution: (a) top, g_{ClO} , g_{ClH} , and n_{ClO} , n_{ClH} ; (b) bottom, g_{PtO} , g_{PtH} , and n_{PtO} , n_{PtH} .

Table 5. Characteristic Values for the Pair Correlation Functions $g_{\alpha\beta}(r)$ for $[\text{PtCl}_6]^{2-}$ in Solution^a

a	b	r_{M1}	$g_{\text{ab}}(r_{\text{M1}})$	r_{m1}	$g_{\text{ab}}(r_{\text{m1}})$	$n(r_{\text{M1}})$	r_{M2}	$g(r_{\text{M2}})$
Cl	O	3.22	1.98	4.45	0.49	8.4	5.74	1.36
Cl	H	2.49	1.34	4.15	0.70	15.2		
Pt	O	4.15	1.67	4.82	0.78	9.8	5.37	1.38
Pt	H	3.29	1.19	3.90	0.72	9.2	4.51	1.23

^a The values of the positions (in Å) of the first and second $g_{\alpha\beta}$ peak maxima (r_{M1}) and minima (r_{m1}) along with the integration numbers of the first peaks are shown.

mately 3.2 Å, indicates the presence of an ordered solvation shell around the complex. Upon inspection of the $\text{Cl}\cdots\text{H}$ distribution, only one broad peak at 2.49 Å is found, which accounts for the interaction of the Cl ligands with the hydrogen atoms of nearby water molecules. This most probable $\text{Cl}\cdots\text{H}$ interatomic distance compares favorably with the DFT water cluster values at 2.46 Å discussed in the preceding section. The sharp $\text{Cl}\cdots\text{O}$ peak and the short $\text{Cl}\cdots\text{H}$ distance both imply that strong, long-lived hydrogen bonds exist between the chlorine ligands and surrounding water molecules. In addition to the $\text{Cl}\cdots\text{O}$ PCF, the $\text{Pt}\cdots\text{H}$ distribution (Figure 3 and Table 5) also exhibits a peak at 3.2 Å, leading us to conclude that the experimentally observed peak at 3.2 Å is in fact a composite of the first $\text{Cl}\cdots\text{O}$ and $\text{Pt}\cdots\text{H}$ peaks. Reconciling the second unassigned X-ray diffraction peak and the PCFs from our computer simulation is less obvious. In the region of ± 1 Å around the measured peak center of 4.9 Å, there are four peaks from our calculated PCFs. A combination of the second $g_{\text{ClO}}(r)$ and $g_{\text{PtH}}(r)$ maxima (at 5.74 and 4.58 Å, respectively) and both $g_{\text{PtO}}(r)$ peaks (at 4.14 and 5.37 Å, respectively) probably account for the unassigned experimentally observed broad peak at 4.9 Å.

$$g_{\alpha\beta}(r) = \frac{1}{4\pi\rho r^2} \frac{dN_{\alpha\beta}(r)}{dr} \quad (4)$$

The presence of a second $g_{\text{ClO}}(r)$ peak at 5.74 Å for the $[\text{PtCl}_6]^{2-}$ solution is likely to be the result of the correlation of chloride ligands with more distant water molecules in the first hydration shell associated with adjacent chloride ligands. The number of solvent atoms in the hydration sphere may be calculated by integrating the first peaks of the $g_{\text{ClO}}(r)$ and $g_{\text{ClH}}(r)$ graphs. This was done for all the PCFs, resulting in running integration numbers $n_{\alpha\beta}(r)$, defined in Eq 5, where ρ_0 is the number density of the atoms of type β .

$$n_{\alpha\beta}(r) = 4\pi\rho_0 \int_0^r g_{\alpha\beta}(r') r'^2 dr \quad (5)$$

The complete list of $g_{\alpha\beta}(r)$ peak data and the corresponding number of correlated atoms $n_{\alpha\beta}(r)$ for that peak are given in Table 5. There are 8 oxygen atoms correlated to the chloride ligands from the first $g_{\text{ClO}}(r)$ peak, and approximately 16 hydrogen atoms. Consequently the first hydration shell for the $[\text{PtCl}_6]^{2-}$ anion comprises on average 8 water molecules. The radially averaged $g_{\text{ClO}}(r)$ distribution presented here results in an isotropic description of the solvation shell. We are at present resolving the simulation data anisotropically for $[\text{PtCl}_6]^{2-}$, $[\text{PdCl}_4]^{2-}$, and $[\text{RhCl}_6]^{3-}$ solutions by applying a novel three-dimensional distribution technique.⁵⁰

6. Conclusions

We have constructed a force field for three PGM chloranionic complexes, $[\text{PtCl}_6]^{2-}$, $[\text{PdCl}_4]^{2-}$, and $[\text{RhCl}_6]^{3-}$, designed for use in computer simulations of metal complex aqueous solutions. Due to the lack of reliable experimental data for the PGM complexes, we used DFT methods to generate structural and spectroscopic data. We tested different functionals and found the LDA approximation to be most suitable for PGM complexes in vacuo. This is in agreement with previous studies.^{5,6} Transition metal complexes are difficult to model using classical approximations. It is for this reason that we chose a small set of complexes to produce a highly specific force field rather than introduce many parameters to accommodate the subtle differences occurring across a range of compounds due to quantum effects, such as the Jahn–Teller distortion and the trans effect. Structural parameters and partial atomic charges were derived from DFT calculations. Values were assigned to the parameters on the basis of two criteria: (1) to reproduce the results of DFT vibrational frequency calculations; (2) to represent the molecular ESP calculated from the electronic wave function as accurately as possible with a point charge model.

The force field presented here produces geometries that compare well with those from DFT calculations on water–metal complex interactions. Furthermore, the results of an MD simulation of $[\text{PtCl}_6]^{2-}$ in water using this force field are in excellent agreement with X-ray diffraction studies of a similar hexachloroplatinate solution. The strong correlation of the peak positions of our PCFs with those from the experimental RDF gives us confidence in the reliability of the force field for PGM chloroanion simulations in aqueous solution.

Acknowledgment. Financial support from the National Research Foundation (South Africa) and the University of Cape Town is gratefully acknowledged.

IC0005745